# Constant threshold resistivity in the metal-insulator transition of VO$_2$

J. Cao,[1,2] W. Fan,[1,3] K. Chen,[4] N. Tamura,[4] M. Kunz,[4] V. Eyert,[5] and J. Wu[1,2,*]

[1]*Department of Materials Science and Engineering, University of California, Berkeley, California 94720, USA*

[2]*Materials Sciences Division, Lawrence Berkeley National Laboratory, Berkeley, California 94720, USA*

[3]*Department of Thermal Science and Energy Engineering, University of Science and Technology of China, Hefei, China*

[4]*Advanced Light Source, Lawrence Berkeley National Laboratory, Berkeley, California 94720, USA*

[5]*Institute for Physics, University of Augsburg, Augsburg 86135, Germany*

We report a constant threshold resistivity observed for the insulating phase of VO$_2$ before it transfers into the metallic phase, regardless of the initial resistivity, transition temperature, and strain state. The value of the threshold resistivity is also comparable for different lattice structures of the insulating phase. Such a constant threshold resistivity suggests that a constant critical free-electron concentration is needed on the insulating side to trigger the insulator-to-metal transition, indicating the electronic nature of the mechanism of the transition.

Strongly correlated electron materials are typically characterized by a variety of phase transitions that occur as a result of competing interactions between charge, spin, orbital, and lattice degrees of freedom. Vanadium dioxide (VO$_2$) is such an example. Free-standing VO$_2$ undergoes a first-order metal-insulator phase transition (MIT) at $T_c^0 = 341$ K from a high-temperature metallic (M) phase to a low-temperature insulating/semiconducting (I) phase.[1] The electronic phase transition is accompanied by a structural change from a tetragonal lattice in the M phase to a monoclinic lattice in the I phase (known as the M1 structure). The I phase features zigzag dimerization of all vanadium atoms along the tetragonal $c$ axis. The MIT occurs when the $t_{2g}$ band that is primarily derived from the vanadium $3d$ states splits. It has been a topic of debate[2] for decades that whether the MIT is fundamentally driven by electron-electron correlation, therefore is a Mott transition, or by electron-lattice interaction, therefore a Peierls transition. An electron correlation assisted Peierls model was also proposed in an attempt to reconcile both mechanisms in VO$_2$.[3] Identification of the driving mechanism in this MIT would help elucidate electron behavior in a wide range of correlated electron materials.[4–6] The controversy is elevated recently by more experimental evidences supporting both mechanisms. The structurally driven MIT was supported by studies using ultrafast spectroscopy on the subvibrational time scale.[7] On the other hand, infrared optical studies of the M phase revealed charge dynamics dominated by electron correlation.[8,9]

The controversy is largely due to poorly understood near-threshold behavior in thin films or bulk crystals, where phase separation and domain formation prevent direct measurement of intrinsic electronic and optical properties.[8] To avoid this complication, single-crystal VO$_2$ nanobeam and microbeam were recently synthesized,[10] where the beam width was comparable to the M/I domain size, allowing electrical and optical characterization at the *single-domain level*.[10–13] Raman spectrum (Fig. 1 inset) shows no phase coexistence in these microbeams in the absence of strain. When the beam is clamped onto a substrate at its two ends and heated up to high temperatures, the VO$_2$ can be forced to move along the M/I phase boundary in the stress-temperature phase space.

The M and I domains align one-dimensionally along the beam. A constant resistivity was observed for the I phase in this configuration.[14,15] The uniaxial strain in Ref. 14, however, is only passively and indirectly introduced by controlling temperature; the probed phase coexisting regime is limited to a narrow range of *tensile* stress. It is much desired to test whether such a constant threshold resistivity is universal over a wider range of phase space extended to *compressive* strain, where the thermodynamically stable I phase of VO$_2$ takes different lattice structure from that in the tensile states (see below). In a recent work, the MIT was activated and continuously modulated by artificially stressing the VO$_2$ microbeams over regions of extraordinarily high strain.[16] The small width and lack of structural defects in these microbeams allowed them to withstand an unprecedentedly high uniaxial strain ($>2.5\%$, as compared to $< \sim 0.1\%$ in the bulk[17]) without plastic deformation or fracture.[16] In this present work we explore the electrical properties of VO$_2$ using this approach. Our experiments reveal that a constant threshold resistivity needs to be reached in the I phase, regardless of its strain state, before it switches into the M state.
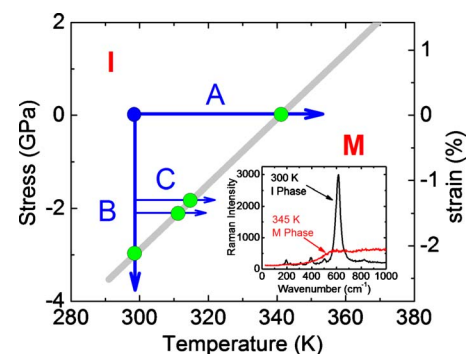


FIG. 1. (Color online) (a) Isobaric, (b) isothermal, and (c) combined sequential processes in the uniaxial stress-temperature phase diagram of VO$_2$ showing phase transition from the I phase to M phase. Dots on the boundary line show schematically the position where the transition threshold is defined. Inset shows Raman spectrum obtained from a strain-free microbeam at two temperatures showing no mixed phase.

The result suggests that a universal and nondegenerate critical carrier concentration is needed to close the gap in VO$_2$.

Owing to the structural change accompanying the MIT from I to M phase, the sample shrinks along the tetragonal $c$-axis direction by $\varepsilon_0 \approx 1\%$.[18] Therefore, uniaxial compressive (or tensile) stress along this direction tends to drive VO$_2$ toward the M (or I) phase. The threshold stress ($\sigma_c$) needed for such transition at temperature $T_C$ follows the uniaxial Clapeyron equation,

$$\frac{d\sigma_c}{dT_c} = \frac{\Delta H}{\varepsilon_0 \cdot T_c}, \tag{1}$$

where $\Delta H$ is the latent heat of the transition. Under linear approximation near $T_c^0$, the solution is $\sigma_c = \alpha(T_c - T_c^0)$, where $\alpha = \Delta H/(\varepsilon_0 T_c^0) = 0.07$ GPa/K established in previous experiments.[16] In Fig. 1 this M-I phase boundary is shown on the temperature ($T$)—stress ($\sigma$) phase diagram. Note that a second insulating phase, known as the M2 phase (labeled as I$_{M2}$ in this Rapid Communication) exists under stress.[17,19] I$_{M2}$ also takes a monoclinic structure, but only half of the vanadium atoms pair up along the $c$-axis direction, and the other vanadium atoms form zigzag chains.[1] Compared to the ambient I phase (I$_{M1}$), in the I$_{M2}$ structure the specimen expands along the $c$-axis direction by 0.3%–0.5%,[18] and therefore can be induced by tensile stress. According to Fig. 1, in ambient condition VO$_2$ is in I state. The M state can be reached either following the route A at constant stress (akin to the isobaric process for a liquid-vapor transition), or following the route B at constant temperature (isothermal process). Moreover, routes A and B can be combined to form sequential processes following the routes C. Unlike previous experiments where stress and temperature variations are either not simultaneously accessible[20] or not separately tunable,[14] in the present work our devices allow investigation of the MIT in the two-dimensional $T$-$\sigma$ phase space by independently varying $T$ and $\sigma$.

Single-crystal VO$_2$ microbeams were synthesized using the vapor transport method reported previously.[10,11] These VO$_2$ beams grow along the tetragonal $c$ axis with rectangular cross section. Using these VO$_2$ beams we patterned devices on bendable Kapton substrates for electric measurements following the methods described before.[16,19] Ohmic contacts were confirmed with four-probe measurements. Figures 2(a)–2(c) show the MIT in such a device (VO$_2$ beam length 6 $\mu$m, width 1.2 $\mu$m, and height 0.8 $\mu$m) driven by temperature increase, compressive stress, and Joule heating, respectively, corresponding to the routes A, B, and C, respectively. In Fig. 2(a) the resistance ($R$) of the VO$_2$ beam is shown as a function of temperature while the device was held at a compressive strain of ~1.4%. With increasing temperature, $R$ decreases exponentially until 320 K, where M domains start to nucleate out of the I phase and cause additional drop in resistance. The device exhibits a hysteresis upon a heating-cooling cycle, typical of first-order phase transition. In contrast to an unconstrained first-order transition where a single, abrupt jump in $R$ is expected, the $R(T)$ curve shows gradual change and ministeps which are caused by the multiple domains during the MIT.[11] Similar behavior
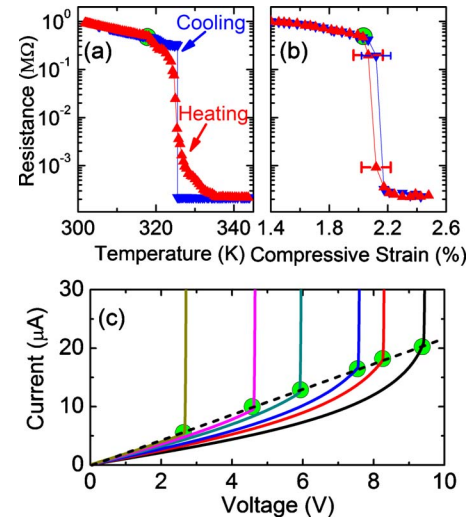


FIG. 2. (Color online) Metal-insulator transition in a VO$_2$ device driven by (a) temperature increase (at 1.4% compressive strain), (b) compressive stress (at 300 K), and (c) Joule heating under different compressive stress. In (c) the uniaxial compressive strain for each $I$-$V$ curve is (from left to right) 1.99%, 1.94%, 1.87%, 1.76%, 1.69%, and 1.58%, respectively. Dots denote the threshold on each of the curves.

of $R$ was observed with the variation in stress. Figure 2(b) shows $R$ as a function of strain at room temperature. $R$ first decreases exponentially until the beam is stressed to a total strain of approximately ~2%, then drops rapidly as M domains grow out of the I phase, and ultimately reaches a full M state at ~2.2% compressive strain. In addition, the MIT can be induced in single VO$_2$ beams by Joule heating.[12,21] The beam is self-heated into the M phase when the bias voltage exceeds a threshold ($V_{th}$) and the experiment was performed at different uniaxial strains [Fig. 2(c)]. With increasing strain, both $V_{th}$ and the current at $V_{th}$ were reduced drastically as expected. An intriguing observation is, however, that the I-phase resistance of the device at the threshold, and consequently the related threshold resistivity ($\rho_{th}$), stays constant over the range of compression, as indicated by the dashed line in Fig. 2(c). The value of $\rho_{th}$ is calculated to be the same (7 $\Omega$ cm) for all routes of MIT shown in Figs. 2(a)–2(c). Note that these experiments were performed from the *same* VO$_2$ microbeam in *strongly compressive* strain state. Attempt to apply tensile stress by convex bending the substrate resulted in mechanical fracture and electrical instability of the electrodes.

In Ref. 14 Wei *et al.* reported a constant $\rho_{th}$ in VO$_2$ along the M-I phase boundary in *tensile* strain state. In this scenario a threshold resistivity $\rho_{th} = 12 \pm 2$ $\Omega$ cm was observed mostly for temperatures above $T_c^0$. It has been established that the triple point where the I$_{M1}$ and I$_{M2}$ phases meet the M phase is very close to the point where stress $\sigma = 0$ and temperature $T = T_c^0$.[17] This suggests that $\rho_{th} = 12 \pm 2$ $\Omega$ cm measured in Ref. 14 is for I$_{M2}$/M transition under tensile strain[13,22] while $\rho_{th} = 7 \pm 2$ $\Omega$ cm measured in the present work is for I$_{M1}$/M transition under compressive strain. These two threshold values are comparable despite the drastically different crystal structures, strain states, and temperatures.

Such an electronic universality over different structures is a clear indication of the electronic origin of the phase transition.

The resistivity in the I-phase depends on temperature primarily through the thermally activated electron concentration,[23,24] $\rho(T) = \rho_0 \exp(E_a/k_B T)$, where $E_a$ is the excitation energy needed. Figure 2(b) shows that $\rho$ depends on stress in a similar exponential way. We therefore write, to first-order approximation, $\rho(T,\sigma) = \rho_0 \exp[(E_a + \gamma\sigma)/k_B T]$, where $\gamma$ is the linear stress coefficient of the excitation energy. Fitting this equation to the I phase part of Figs. 2(a) and 2(b), we determined $E_a = 0.36 \pm 0.01$ eV and $\gamma = -0.015 \pm 0.002$ eV/GPa for this device. This value of $E_a$ is comparable to those obtained on VO$_2$ microbeams (0.3 eV) (Ref. 14) and on VO$_2$ bulk (0.45 eV).[24,25] Similar to the effect of applying hydrostatic pressure,[26] uniaxial stress would shift the conduction-band minimum with respect to the dopant energy level, thus effectively changing $E_a$. The value of $\gamma$ also agrees with the value ($-0.012$ eV/GPa) calculated from $d \ln R/d\sigma$ reported in literature.[20] It is seen from the expression of $\rho(T,\sigma)$ that more free electrons can be excited by either increasing temperature or, independently, compressing the lattice, resulting in a decrease in the resistivity. At sufficiently high temperature or large compression, the I phase is no longer thermodynamically stable, such that VO$_2$ undergoes the MIT and transfers to the M state. The threshold temperature or stress for this to occur is given by the Clapeyron relation in Eq. (1). This relation defines $\rho_{th}$ through $\rho(T,\sigma)$ as $\rho_{th} = \rho[T, \sigma_c(T)]$. To see the constancy of $\rho_{th}$, we calculate its relative change as the system moves along the M-I boundary,

$$\frac{\Delta\rho_{th}}{\rho_{th}} = \frac{\alpha\gamma T_c^0 - E_a}{k_B T_c^0} \times \frac{\Delta T_c}{T_c^0}. \qquad (2)$$

Using the values and uncertainties of $\gamma$ and $E_a$ obtained in our experiment, the first factor on the right-hand side of Eq. (2) is calculated to be between $-0.37$ and $0.37$. Therefore, even for MIT occurring at room temperature ($T_c = 300$ K), very far from the natural MIT temperature $T_c^0 = 341$ K, Eq. (2) yields $|\Delta\rho_{th}|/\rho_{th} < 5\%$. This shows that the MIT indeed occurs at a constant $\rho_{th} = \rho_0 e^{\alpha\gamma/k_B} \approx 7$ $\Omega$ cm. Although $T$ and $\sigma$ are two independent experimental parameters, when both are being tuned to the threshold of MIT, the effect of increasing thermal excitation is exactly counteracted by the effect of bandgap widening, such that a constant $\rho_{th}$ is maintained. We note that the range of strain explored in this study ($>2\%$) is more than an order of magnitude higher than that was previously attained in the bulk,[17] therefore the constancy of $\rho_{th}$ is over a remarkably wide region in the phase diagram.

Figure 3 shows the values of $\rho_{th}$ obtained from the transition curves in Figs. 2(a)–2(c). We also measured $\rho_{th}$ of several other devices fabricated directly on the growth chip. In these devices the VO$_2$ beams formed at high temperatures ($\sim 950$ °C) on a molten SiO$_2$ surface; when cooled to lower temperatures, the SiO$_2$ solidified and the VO$_2$ beams were entirely pinned onto the SiO$_2$ surface.[10,11] Depending on local conditions during this pinning process, these beams could be clamped in different strain states varying from beam to
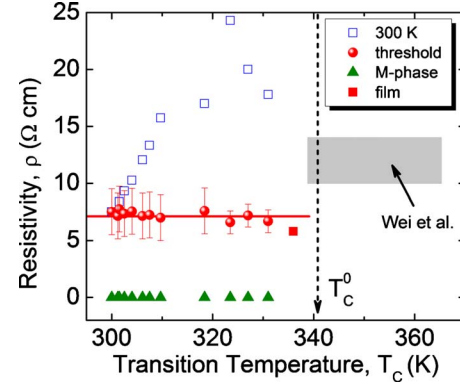


FIG. 3. (Color online) Measured resistivity of VO$_2$ microbeams at 300 K, at the threshold, and in M-phase, respectively. The error is mostly from uncertainties in determining the effective height and length of the microbeams. Also shown is the apparent threshold resistivity from a VO$_2$ thin film (Ref. 26), and the threshold resistivity from tensile strained VO$_2$ microbeams by Wei _et al._ (Ref. 14). The horizontal line shows the constancy of $\rho_{th}$ in I phase, and the vertical line divides tensile (right) from compressive (left) regions.

beam. When temperature $T$ is increased and reaches $T_c$ in these devices, beam resistance $R$ starts to deviate from the Arrhenius dependence on $T$, indicative of the first M domain emerging along the beam.[11] The resistivity $\rho$ at $T_c$ is defined as $\rho_{th}$. Afterwards $R$ behaves in a complicated way determined by the inhomogeneous strain distribution in this clamped VO$_2$/SiO$_2$ system.[11] In this way $\rho_{th}$ from different VO$_2$ microbeams can be evaluated and plotted together in Fig. 3. It can be seen that despite they have different $T_c$ and room temperature $\rho$, their $\rho_{th}$ all fall onto the constant $\rho_{th}$ line.

We note that a range of $\rho_{th}$ between 0.2 and 12 $\Omega$ cm was reported on bulk[23] or thin films[27] of VO$_2$. The difference in $\rho_{th}$ from ours might be caused by different electron mobility (as opposed to different $n_{th}$), or by overlooked M-phase domains that nucleate before the apparent threshold on the measured $\rho(T)$ curve due to inhomogeneous strain or doping. Hydrostatic pressure experiments on VO$_2$ bulk crystals showed convergence of $\rho$ to $\sim 11$ $\Omega$ cm as the MIT is approached by increasing temperature, independent of the pressure applied.[26] This behavior is consistent with the constant $\rho_{th}$ observed in our uniaxial stressing experiments. In nondegenerate doping such as in the I-phase VO$_2$, electron concentration ($n$) is expected to be much more sensitive than mobility ($\mu$) to strain and temperature.[23,27] The constant $\rho_{th}$ therefore implies a constant threshold $n$, defined as $n_{th}$, for the I-phase VO$_2$ beam to undergo the transition to M phase. Assuming a mobility of $\mu = 0.11$ cm$^2$/V s reported on VO$_2$ thin films,[27] we estimate $n_{th}$ in our microbeams to be $8 \times 10^{18}$ cm$^{-3}$.

Such a constant $n_{th}$ has deep implications to the physics of the MIT. According to all existing calculations [local-density approximation (LDA), LDA+$U$, LDA+dynamical mean field theory] and a great variety of experimental data, there is a consensus that the MIT involves drastic changes in orbital occupation. In particular while the M phase is characterized by a nearly equal occupation of all three $t_{2g}$ orbitals leading

to a nearly isotropic charge distribution at the V sites, strong orbital ordering is found for the $I_{M1}$ phase leaving the $\pi^*$ bands unoccupied, and the $d_\parallel$ band is split and half filled causing a predominantly one-dimensional charge distribution.[1,3,28,29] LDA (Ref. [1]) and new LDA+$U$ calculations using the full-potential augmented spherical wave method reveal a very similar scenario for the $I_{M2}$ phase. As a consequence, the small $n_{th}$ will populate predominantly the $\pi^*$ orbitals. Starting from the insulating phase, excitation of carriers into the $\pi^*$ bands leads to a downshift of these bands relative to the oxygen-dominated $\pi$ bands and the antiferroelectric zigzag distortion will become energetically less favorable. As a consequence, via the electrostatic coupling between the V-V dimerization on one vanadium chain and the zigzag displacement on the neighboring chains,[1,30–32] the reduction in the antiferroelectric distortion will reduce the V-V dimerization and trigger the structural transition. At the same time, the energy separation between the $d_\parallel$ and $d_\parallel^*$ will shrink and so will the energy separation between the $d_\parallel$ and $\pi^*$ bands (band gap). This in turn facilitates excitation of even more electrons until, finally, the electronic system collapses and the M phase occurs. The constant $n_{th}$ thus gives strong hints that the insulator-to-metal phase transition is initiated by a reduction in the antiferroelectric distortion due to increasing population of the $\pi^*$ bands, and this is a universal behavior valid for both insulating phases of $VO_2$. We believe that the single-domain investigation demonstrated here can be extended to other strongly correlated electron nanomaterials to uncover intrinsic physical properties unattainable in the bulk.

In summary, we measured electrical conduction of single-crystal $VO_2$ microbeams across the metal-insulator transition at various stress and temperatures and observed a universal resistivity for the insulating phase on the verge of the transition. The crystallinity, size, and geometry of the microbeams allow for such studies over a wide range of strain and temperatures in the phase space. The threshold resistivity is independent of the initial resistivity, transition temperature, and strain of the sample. Different lattice structures also exhibit comparable threshold resistivities. The constant threshold resistivity indicates that the transition to metallic phase occurs only when electronic screening reaches a critical strength, suggesting the electronic origin of the transition.

*Author to whom correspondence should be addressed; wuj@berkeley.edu

[1] V. Eyert, Ann. Phys. **11**, 650 (2002).

[2] R. M. Wentzcovitch, W. W. Schulz, and P. B. Allen, Phys. Rev. Lett. **72**, 3389 (1994).

[3] S. Biermann, A. Poteryaev, A. I. Lichtenstein, and A. Georges, Phys. Rev. Lett. **94**, 026404 (2005).

[4] E. Dagotto, Science **309**, 257 (2005).

[5] P. Limelette *et al.*, Science **302**, 89 (2003).

[6] M. C. Cha, M. P. A. Fisher, S. M. Girvin, M. Wallin, and A. P. Young, Phys. Rev. B **44**, 6883 (1991).

[7] A. Cavalleri, M. Rini, H. H. W. Chong, S. Fourmaux, T. E. Glover, P. A. Heimann, J. C. Kieffer, and R. W. Schoenlein, Phys. Rev. Lett. **95**, 067405 (2005).

[8] M. M. Qazilbash *et al.*, Science **318**, 1750 (2007).

[9] M. M. Qazilbash, K. S. Burch, D. Whisler, D. Shrekenhamer, B. G. Chae, H. T. Kim, and D. N. Basov, Phys. Rev. B **74**, 205118 (2006).

[10] B. S. Guiton *et al.*, J. Am. Chem. Soc. **127**, 498 (2005).

[11] J. Wu *et al.*, Nano Lett. **6**, 2313 (2006).

[12] Q. Gu *et al.*, Nano Lett. **7**, 363 (2007).

[13] S. Zhang, J. Y. Chou, and L. J. Lauhon, Nano Lett. **9**, 4527 (2009).

[14] J. Wei *et al.*, Nat. Nanotechnol. **4**, 420 (2009).

[15] D. Natelson, Nat. Nanotechnol. **4**, 406 (2009).

[16] J. Cao *et al.*, Nat. Nanotechnol. **4**, 732 (2009).

[17] J. P. Pouget *et al.*, Phys. Rev. Lett. **35**, 873 (1975).

[18] M. Marezio *et al.*, Phys. Rev. B **5**, 2541 (1972).

[19] J. Cao *et al.*, Nano Lett. **10**, 2667 (2010).

[20] L. A. Ladd and W. Paul, Solid State Commun. **7**, 425 (1969).

[21] E. Strelcov, Y. Lilach, and A. Kolmakov, Nano Lett. **9**, 2322 (2009).

[22] A. C. Jones, S. Berweger, J. Wei, D. Cobden, and M. B. Raschke, Nano Lett. **10**, 1574 (2010).

[23] C. N. Berglund and H. J. Guggenheim, Phys. Rev. **185**, 1022 (1969).

[24] W. H. Rosevear and W. Paul, Phys. Rev. B **7**, 2109 (1973).

[25] A. Zylbersztejn and N. F. Mott, Phys. Rev. B **11**, 4383 (1975).

[26] C. N. Berglund and A. Jayarama, Phys. Rev. **185**, 1034 (1969).

[27] D. Ruzmetov, D. Heiman, B. B. Claflin, V. Narayanamurti, and S. Ramanathan, Phys. Rev. B **79**, 153107 (2009).

[28] A. Liebsch, H. Ishida, and G. Bihlmayer, Phys. Rev. B **71**, 085109 (2005).

[29] M. A. Korotin, N. A. Skorikov, and V. I. Anisimov, Phys. Met. Metallogr. **94**, 17 (2002).

[30] J. P. Pouget *et al.*, Phys. Rev. B **10**, 1801 (1974).

[31] D. Paquet and P. Leroux-Hugon, Phys. Rev. B **22**, 5284 (1980).

[32] T. M. Rice, H. Launois, and J. P. Pouget, Phys. Rev. Lett. **73**, 3042 (1994).